IRAQI JOURNAL OF MATERIALS
Volume (4) Issue (3) July-September 2025, pp. 101-108

Spin-Orbit Splitting Dependent Single-Colour Multiphoton Absorption Spectroscopy and Spin Orientation in Noncentrosymmetric Semiconductors with Narrow to Wide Bandgaps

M. Idrish Miah

Department of Physics, University of Chittagong, Chittagong–4331, BANGLADESH
Email: m.idrish.miah@cu.ac.bd

Abstract
We study the spin-orbit splitting dependent single-coloured multiphoton absorption spectroscopy and spin orientation in noncentrosymmetric InSb, GaSb and ZnSe by calculations of spectra for these compounds. Calculations are focused on the photon-frequency dependent absorption and spin generation on the basis of the Kane model. It is found that the electronic spin polarization (P) depends on the absorption scheme of the spectroscopy as well as pumping direction and excess photon energy of exciting carriers. A maximum value of P is found to be about 55%. The P reaches its maximum value at the lower energy and sustains shorter energy range for InSb. The P is also found to depend on the bandgap energy and spin-orbit splitting. The results show that due to a much longer absorption depth multiphoton absorption enhances the spin generation and thus spin polarization.

Keywords: Optical selection; Spin-orbit splitting; Spin polarization; Spectroscopy; Semiconductors
Received: 19 April 2025; **Revised:** 21 June 2025; **Accepted:** 28 June 2025; **Published:** 1 July 2025

1. Introduction

Spintronics is the use of a fundamental property of particles known as spin for information processing. In many ways, spintronics is analogous to electronics, which instead uses the electrical charge on an electron. Carrying information in both the charge and spin of an electron potentially offers devices with a greater diversity of functionality. This approach to electronics is emerging that is based on the spin sates of the electron rather than on its charge as in traditional electronics [1-5]. This field was initiated by the studies of Baibich et al [6] and Binasch et al [7] who showed that a system of alternating ferromagnetic and nonmagnetic metal interlayers, with appropriate construction and an applied magnetic field, could change an electrical resistance from small (with parallel magnetizations) to large (with antiparallel magnetizations) and the changes could be large enough to be called a giant magnetoresistance (GMR). The GMR effect found its way to computer applications when IBM incorporated a magnetic device known as a ‘spin-valve’ into the read-head of hard disks. This spin technology based on metals (metallic spintronics) was established, and there is nothing much to do with.

However, as semiconductors have more flexibility of controlling both charge and spin, semiconductor spintronics has a huge potential of applications and devices. Spintronics is now a multidisciplinary field involving physics, chemistry, materials science and engineering and has widely been studied in the semiconductors [8,9]. Electronic spin-polarization and its reliable transport in semiconductors is an essential condition to be achieved for semiconductor spintronics. For this a high degree of spin polarization is required.

Optically generated spin polarization in semiconductors have been studied [10-12]. Recently, we studied two-photon spin generation GaAs both theoretically and experimentally [13,14]. Here, in the present investigation, we study the electronic spin orientation and polarization in narrow to larger fundamental bandgap semiconductors InSb, GaSb and ZnSe on the basis of the eight-band Kane model. These compounds are noncentrosymmetric with cubic structures. InSb and GaSb are the III-V group and ZnSe is the II-VI group compounds. InSb (0.235 eV), GaSb (0.813 eV) and ZnSe (2.820 eV) have, respectively, narrow, small and wide bandgap semiconductors. We consider the high frequency limit [13] in our calculation. It is found that the electron spin polarization depends on the excitation

scheme of the spectroscopy, the excess photon energy as well as bandgap energy and spin-orbit splitting. In this study, a high spin polarization of maximum 55% is obtained.

2. Energy Bands and spin orientation

Optical spin generation utilizes eight-band Kane model and optical selection rules for transitions, as depicted in Fig. (1). According to the optical selection rules, transition probability from the valence band heavy-hole (HH) state to the conduction band (CB) is three times larger than from the light-hole (LH) state. As the LH transition generates opposite spins, the optical excitation produces a 3:1 ratio of to spin-up to spin-down CB electrons for a left (right) circularly polarized light $\sigma^-(\sigma^+)$ provided that the photon energy is low enough to avoid exciting carriers from the split-off band. If $n_\uparrow$($n_\downarrow$) is the number of electrons with spin up (down), the degree of spin (P) polarization, calculated from the definition

$$P(\vec{r},t)=\frac{n_\uparrow(\vec{r},t)-n_\downarrow(\vec{r},t)}{n_\uparrow(\vec{r},t)+n_\downarrow(\vec{r},t)} \quad (1)$$

gives a maximum (3+1)/(3-1)=0.5 or 50% spin polarization in bulk semiconductors. A 50% spin polarization has not yet been obtained by an optical experiment in a bulk material. In a low-dimensional structure (e.g. quantum well), as the degeneracy of HH and LH bands is removed, the optical excitation of the HH band produces a maximum P= 1 (100%). However, recent studies with multiphoton excitation and full-band calculations show that more than 50% spin polarization could be achieved in some semiconductor materials [13,14]. Optical excitation with a σ^+(σ^-) orients spins along the direction parallel (antiparallel) to the direction of the light propagation.

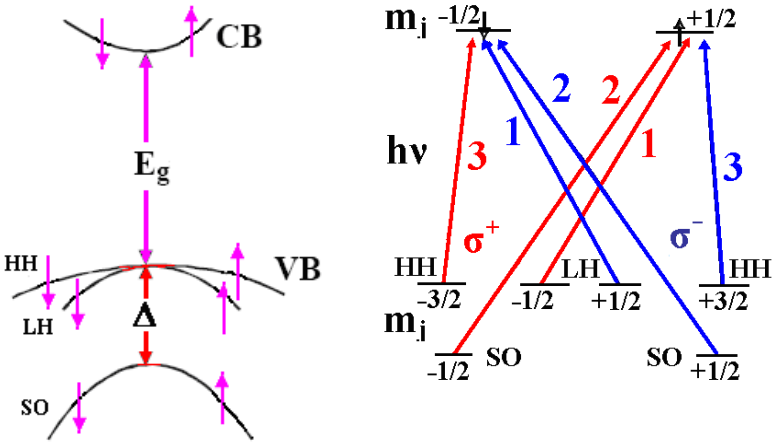

Fig. (1) (Left) Eight band model: A scheme showing the heavy-hole (HH), light-hole (LH) and split-off (SO) bands of a semiconductor. The eight band-states (counting each spin state: spin up ↑ or spin down, ↓) comprise six *p*-like valence band (VB) states (HH, LH and SO bands) and two *s*-like conduction band (CB) states. (Right) Selection rules for transitions: Numbers 1, 2, and 3, respectively, denote transition probabilities for LH, SO and HH valence band (VB) to CB

As a multiphoton process, if we consider the simultaneous absorption of two-photon with different colours, then the absorption condition is

$$E_C > (\hbar\omega_1 + \hbar\omega_2) > E_g \quad (2)$$

Where $E_C=E_g+\Delta$ is the SO to the CB energy, E_g is the energy gap at k =0 (the fundamental bandgap) and $E_{\omega1,\omega2}=\hbar\omega_1+\hbar\omega_2$ is the two-photon energy. However, for single coloured two photons the one-photon and two-photon energies are $E_\omega=\hbar\omega$ and $E_{\omega2}=\hbar2\omega$ respectively. We consider here the later case. An illustration of the one-photon and two-photon excitation schemes showing the excitation pulse for one-photon (ω) and two-photon (2ω) coupling the initial and final states in the VB and CB bands is given in Fig. 2, where $E_p=\hbar\omega_p$ is the probe beam energy. As can be seen, the two-photon pump beam takes a photon of frequency half. The probe pulse (ω_p) tuned to the band gap excitation resonance ($\hbar\omega_p\approx E_g$)

ISSN (print) 2958-8960 (online) 3006-6042 Printed in IRAQ

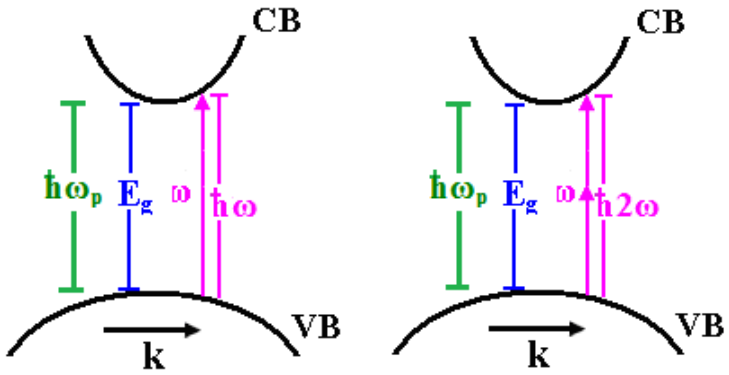

Fig. (2) One-photon and two-photon spectroscopy: An illustration of the one-photon (left) and two-photon (right) excitation schemes showing the excitation pulse for one-photon (ω) and two-photon (2ω) coupling the initial and final states in the VB and CB bands. The probe pulse (ω_p) tuned to the band gap (E_g) excitation resonance. Here $E_\omega=\hbar\omega$, $E_{2\omega}=\hbar 2\omega$, and $E_p=\hbar\omega_p$ are the one-photon, two-photon pump and probe beam energies respectively. The two-photon pump beam takes a photon of frequency half

3. Theoretical model and calculations

We estimate the electronic spin-polarization by calculating the both one-photon and two-photon photo-generation rates of electron spin density for InSb, GaSb and ZnSe compounds with E_g ranging from 0.235 to 2.820 eV. In the calculations, in order to neglect the many-body and electron-phonon interactions, we consider the low frequency limit in the perturbation theory [15]. As optically excited hole spin relaxation is extremely fast, their polarization is effectively zero, and can be neglected. For an electric field E the two-photon spin generation rate can be written as

$$\dot{\boldsymbol{\Omega}} = \chi^{ijklm} E_\omega^j E_\omega^k E_\omega^{l^*} E_\omega^{m^*}$$

where χ^{ijklm} is a fifth rank pseudotensor symmetric on exchange of indices, which for the doubly degenerate band case is obtained from the Fermi's golden as [13,17]

$$\dot{\boldsymbol{\Omega}} = \left(\frac{2\pi}{V}\right)\sum_{c,c',v,\mathbf{k}}\langle c\mathbf{k}|\hat{\boldsymbol{\Omega}}|c'\mathbf{k}\rangle\, \mathrm{S}^{(2)^*}_{c',v,\mathbf{k}}\mathrm{S}^{(2)}_{c,v,\mathbf{k}}\Lambda_{\mathbf{k}} \qquad (3)$$

where the dot on the symbol denotes its time derivative, V is the normalized volume, $\hat{\boldsymbol{\Omega}}$ is the spin operator, $|nk\rangle$ is a Bloch state with energy $\hbar\omega_n(\mathbf{k})$ and

$$\Lambda_{\mathbf{k}} = \frac{1}{2}\left[\delta\left|2\omega-\omega_{cv}(\mathbf{k})\right|+\delta\left|2\omega-\omega_{cv'}(\mathbf{k})\right|\right] \qquad (4)$$

The two-photon absorbed amplitude is

$$\mathrm{S}^{(2)}_{\mathrm{c,v,k}} = (e/E_\omega)^2\sum_n\{\mathbf{E}_\omega.\mathbf{v}_{c,n}(\mathbf{k})\}\{\mathbf{E}_\omega.\mathbf{v}_{n,v}(\mathbf{k})\}/\{\omega_{nv}-\omega(\mathbf{k})\} \qquad (5)$$

The two-photon absorption (2PA) is incorporated by the frequency term 2ω in Eq. (4). Here $v_{n,m}(\mathbf{k}) = \langle n\mathbf{k}|\hat{v}|m\mathbf{k}\rangle$ and $\hat{v}$ is the velocity operator. Similarly, the optical generation rate of the 2PA electron-hole pairs can be obtained as

$$\dot{n} = \left(\frac{2\pi}{V}\right)\sum_{c,c',v,\mathbf{k}}\left|\mathrm{S}^{(2)}_{c,v,\mathbf{k}}\right|^2\delta\{2\omega-\omega_{cv}(\mathbf{k})\} \qquad (6)$$

We arrive at the following relation for the light incident along $\hat{z}$, specified by polar angles θ and φ relative to the cubic axes,

$$\boldsymbol{\Omega}\dot{\times}\hat{z} = \mp\chi_{2A}|\mathbf{E}_\omega|^4\left[1+\frac{(2\chi_{2B}-\chi_{2A})\{sin^2(2\theta)+sin^4(\theta)sin^2(2\varphi)\}}{4\chi_{2A}}\right] \qquad (7)$$

The angular term of this equation $a_p(\theta,\varphi)=\sin^2(2\theta)+\sin^4(2\theta)\sin^2(2\varphi)$ is an important function, which shows the cubic anisotropy in pumping, i.e. the angular dependence of pumping in spin-excitation in the cubic system. The term $a_p(\theta,\varphi)$ as a function of θ and φ is plotted in Fig. (3), where the cubic anisotropic behaviour is clearly seen.

ISSN (print) 2958-8960 (online) 3006-6042 Printed in IRAQ

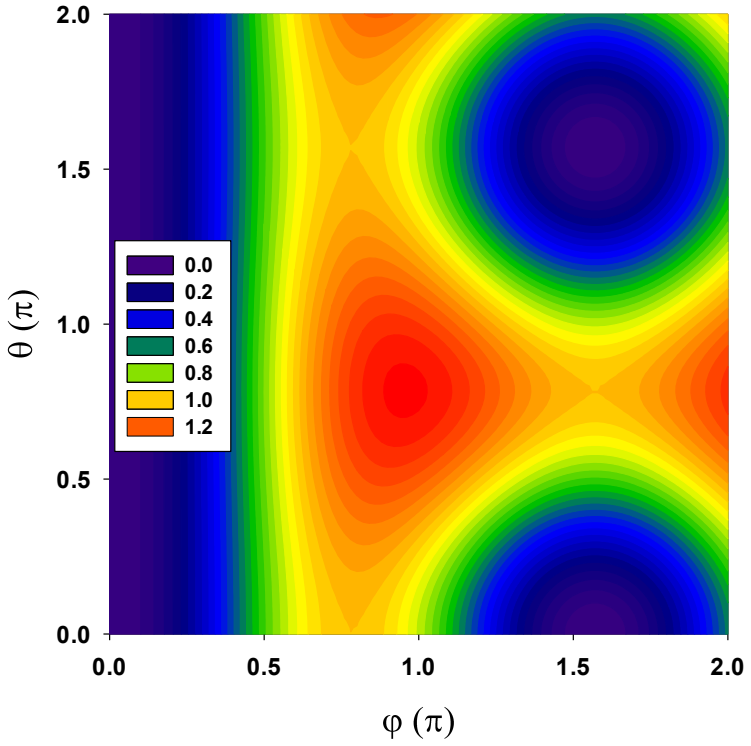

Fig. (3) The contour plot of $a_p(\theta,\varphi)$ as a function of θ and φ which shows the variation of spin generation due to the anisotropy of pumping.

In order to calculate the spin polarization we first calculate the interband transition matrix elements using the eight-band model, as shown in Fig. (1). The parameter-values used for this calculation are taken from [16,17]. Kane wave functions [18] for CB and VB bands in the k.p approximation are

$$\varphi_{c\uparrow} = a_c(iS_\downarrow) + b_c\left\{\frac{(X-iY)_\uparrow}{\sqrt{2}}\right\} + c_c Z_\downarrow \tag{8}$$

$$\varphi_{c\downarrow} = a_c(iS_\uparrow) + b_c\left\{-\frac{(X+iY)_\downarrow}{\sqrt{2}}\right\} + c_c Z_\uparrow \tag{9}$$

$$\varphi_{1\uparrow} = \frac{(X+iY)_\uparrow}{\sqrt{2}} \tag{10}$$

$$\varphi_{1\downarrow} = \frac{(X-iY)_\downarrow}{\sqrt{2}} \tag{11}$$

$$\varphi_{2\uparrow} = a_2(iS_\downarrow) + b_2\left\{\frac{(X-iY)_\uparrow}{\sqrt{2}}\right\} + c_2 Z_\downarrow \tag{12}$$

$$\varphi_{2\downarrow} = a_2(iS_\uparrow) + b_2\left\{-\frac{(X+iY)_\downarrow}{\sqrt{2}}\right\} + c_2 Z_\uparrow \tag{13}$$

$$\varphi_{3\uparrow} = a_3(iS_\downarrow) + b_3\left\{\frac{(X+iY)_\uparrow}{\sqrt{2}}\right\} + c_3 Z_\downarrow \tag{14}$$

$$\varphi_{3\downarrow} = a_3(iS_\uparrow) + b_3\left\{-\frac{(X+iY)_\downarrow}{\sqrt{2}}\right\} + c_3 Z_\uparrow \tag{15}$$

where *c,* 1, 2 and 3 denote CB, HH, LH and SO bands respectively for up (↑) and down (↓) spins. The basis functions *X, Y, Z* and *S* refer to a coordinate system depending on k. The coefficients *a, b* and *c* also depends on k, and for small value of *k* they are approximately

$$a_c = 1,$$

$$b_c = \frac{\sqrt{2}}{3}\frac{p\hbar}{mE_g(1+\zeta)},$$

$$c_c = \frac{p\hbar k}{mE_g}\frac{E_g+2\Delta/3}{E_C},$$

$$a_2 = -\sqrt{\frac{2}{3}}\frac{p\hbar}{mE_g},$$

$$b_2 = 1/\sqrt{3},$$

$$c_2 = \sqrt{2/3},$$

$$a_3 = \frac{1}{\sqrt{3}}\frac{p\hbar}{mE_C},$$

$$b_3 = \sqrt{2/3},$$

$$c_3 = -1/\sqrt{3}$$

with

$$p = \langle iS|p_z|Z\rangle = \sqrt{\frac{3m^2}{2}\left\{\frac{1}{m^*}-\frac{1}{m}\right\}\frac{E_gE_C}{3E_g+2\Delta}} \quad (16)$$

where $\zeta = E_g/\Delta$, p is the electron momentum operator originated from the interacting Hamiltonian of the light field and m^* is the electron effective mass of the CB. For $k = 0$ they reduces to the values as given in Table I of Ref. [15] for the Kane wave functions. As for example, for the $k = 0$ case, the states $|J, m_j\rangle$ for the spin degenerate two conduction bands are

$$\left|\frac{1}{2},\frac{1}{2}\right\rangle \equiv |S_\uparrow\rangle \quad (17a)$$

$$\left|\frac{1}{2},-\frac{1}{2}\right\rangle \equiv |S_\downarrow\rangle \quad (17b)$$

and similarly for the others. Using these wave functions, transition matrix elements were calculated. In the 2PA process the final state involves a conduction electron and a hole. The electron may be either one of the conduction bands (up and down states) $c\uparrow$ and down $c\downarrow$, and the hole may be in one of the six valence bands (Fig. 1). We finally obtain the expression for the electronic spin polarization *P*, defined in Eq. (1), as $P = -2(\dot{\Omega}\cdot\hat{z})/(\hbar\dot{n})$. The polarization *P* due to one-photon excitation is obtained by replacing the frequency term 2ω by ω and the two-photon amplitude by the one-photon amplitude in Eq. (4).

4. Results and Discussion

Electron spin polarization as a function of excess photon energy for multiphoton excitations was calculated for semiconductors InSb, GaSb and ZnSe. The calculated results are shown in figures (4) and (5), where the spin polarization is plotted as a function of the excess photon energy $\Delta E_\omega = \hbar\omega - \hbar\omega_p \approx \hbar\omega - E_g$ and $\Delta E_{2\omega} = 2\hbar\omega - \hbar\omega_p \approx 2\hbar\omega - E_g$, respectively, for the one-photon and two-photon excitations. As expected, the spin polarization *P* increases with the excess photon energy for the lower excess energy and remains almost constant up to ~200 meV for GaSb and ZnSe and then decreases. The decrease is very pronounced for InSb. The *P* reaches its maximum value at the lower energy and sustains shorter

 ISSN (print) 2958-8960 (online) 3006-6042 Printed in IRAQ

energy range for InSb. The maximum value of *P* is about 55% for the two-photon excitation. The *P* reaches its maximum value at the lower energy and sustains shorter energy range for InSb.

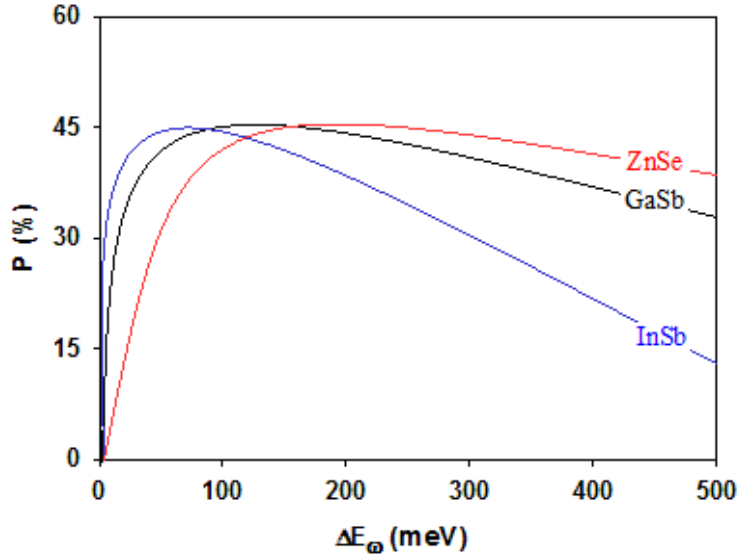

Fig. (4) Spin-polarization as a function of excess photon energy $\Delta E_\omega \approx E_\omega - E_g = \hbar\omega - E_g$ excited by one-photon for InSb, GaSb and ZnSe

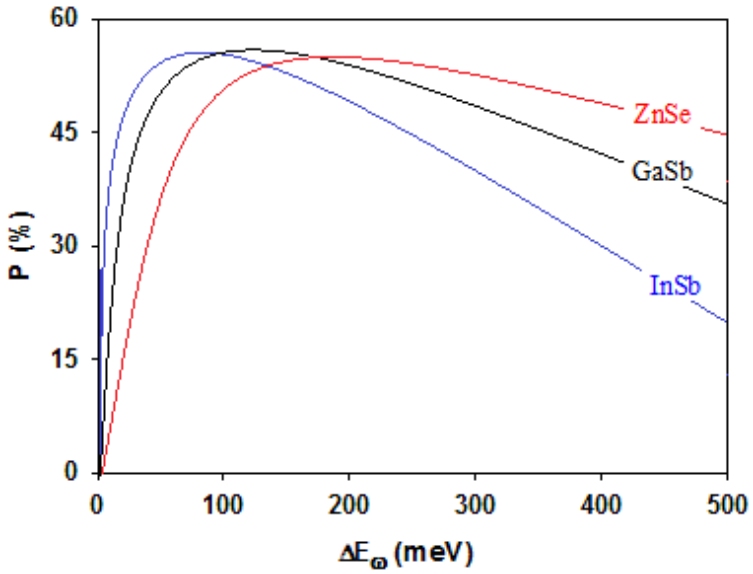

Fig. (5) Spin-polarization as a function of excess photon energy $\Delta E_{2\omega} \approx E_{2\omega} - E_g = \hbar 2\omega - E_g$ excited by two-photon for InSb, GaSb and ZnSe

For the higher excess energy, the polarization decreases rapidly due to the mixture of LH and HH states with the SO valence band states which have an opposite sign. The LH and SO band transitions create the same electron spin orientation and the sum of their inter-band matrix elements is equal to the HH inter-band dipole-transition matrix element. There is still a sizeable degree of electron spin polarization even at excess energy higher than the spin-orbit splitting energy. The results agree well with those for GaAs [13,14].

Although the maximum optical spin-polarization for an unstrained bulk sample is expected to be much more in the present theory, the maximum has experimentally been observed to be less because of the unexciting carriers in the bottom of a bulk. In a bulk sample there might have some background unpolarized electrons, which might not be excited by single-photon excitation [19]. For an optically generated electron density $n(0)=n_\downarrow(0)+n_\uparrow(0)$, there is a background density of unpolarized electrons in

ISSN (print) 2958-8960 (online) 3006-6042 Printed in IRAQ

bulk materials. However, *P* obtained spectroscopically with a single-photon excitation is much less, not more than 40% [20].

On a comparison between figures (4) and (5), it can be seen that a two-photon excitation enhances the spin polarization. This is because it takes the advantages over one-photon spin spectroscopy due to a much longer absorption depth, which allows spin excitation in the deep level, i.e. throughout the volume of a thin bulk sample [21-23].

It thus can be concluded that due to a much longer absorption depth highly spin-polarized electrons can be produced optically by the two-photon excitation of the bulk semiconductors. However, the spin polarization would decay with time due to the randomization of the initial spin polarization by the Dyakonov-Perel (DP) spin relaxation mechanism [2]. The DP spin relaxation occurs in semiconductors lacking inversion symmetry in noncentrosymetric crystals due to the spin precession about an intrinsic magnetic field induced by the presence of the SO interaction $H_{SO}=(\hbar/2)\mathbf{\Omega}.\mathbf{b}_{\mathbf{eff}}$, where the effective single-electron Hamiltonian $H=H_0+H_{SO}$ includes the SO interaction term (SO Hamiltonian, H_{SO}). The self-consistent electron Hamiltonian in the Hartree approximation accounts for the interactions with impurities and phonons as well. The effective magnetic field, given near the bottom of the *Γ*-valley of the cubic structure [24]

$$\mathbf{b}_{\text{eff}} = \gamma\left[k_x(k_y^2-k_z^2)\hat{x}+k_y(k_z^2-k_x^2)\hat{y}+k_z(k_x^2-k_y^2)\hat{z}\right] \quad (18)$$

is a vector depending on the orientation of the electron momentum vector with respect to the crystal axes xyz and causes the electron spin to process, where k_i (i = x, y and z) are the components of the electron wave vector and γ is the SO coupling coefficient and is given by

$$\gamma = \frac{\zeta\hbar^2}{\sqrt{2(m^*)^3E_g}}\left\{1-\frac{E(\mathbf{k})}{E_g}\frac{9-7\eta+2\eta^2}{3-\eta}\right\} \quad (19)$$

where ξ is a dimensionless material-specific parameter which gives the magnitude of the SO splitting and $\eta=\Delta/E_C$. The DP spin processes according to the quantum-mechanical description, like of the equation of motion $\dot{\mathbf{\Omega}} = \mathbf{b}_{\mathbf{eff}} \times \mathbf{\Omega}$. The scattering reorients the direction of the procession axis, making the effective magnetic field random and trajectory dependent, which leads to spin dephasing or relaxation.

The spin polarization *P* as a function of SO slitting Δ for the excess photon energy of 200 meV, excited by one-photon and two-photon for InSb, GaSb and ZnSe is shown in Fig. (6). As can be seen, *P* decreases with Δ for one-photon and two-photon excitations, while *P* increases with *ζ*, the ratio of the bandgap energy to the SO slitting (Fig. 7). The *ζ* of InSb, GaSb and ZnSe are 6.997, 1.084 and 0.293 respectively, which means that maximum *P* is observed for InSb. This might be due the possibility of exciting carriers from the SO bands, as discussed earlier.

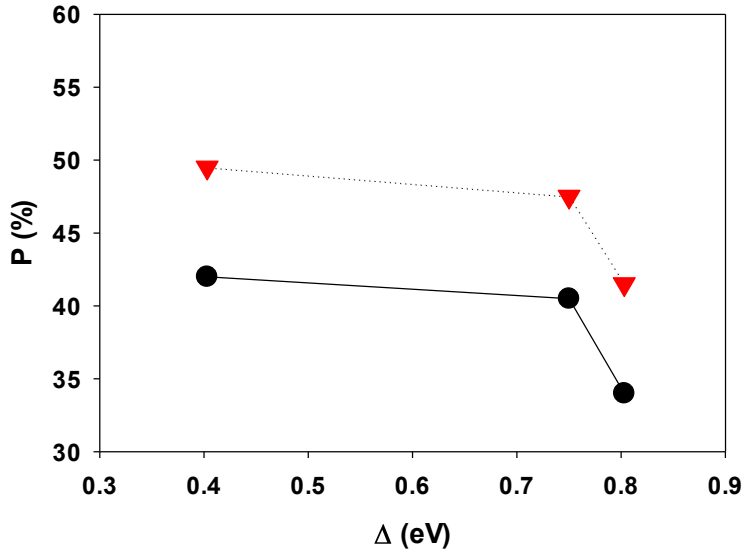

Fig. (6) Spin-polarization as a function of Δ for the excess photon energy of 200 meV, excited by one-photon (circle) and two-photon (triangle) excitations. The Δ of InSb, GaSb and ZnSe are 0.235 eV, 0.813 eV and 2.820 eV respectively

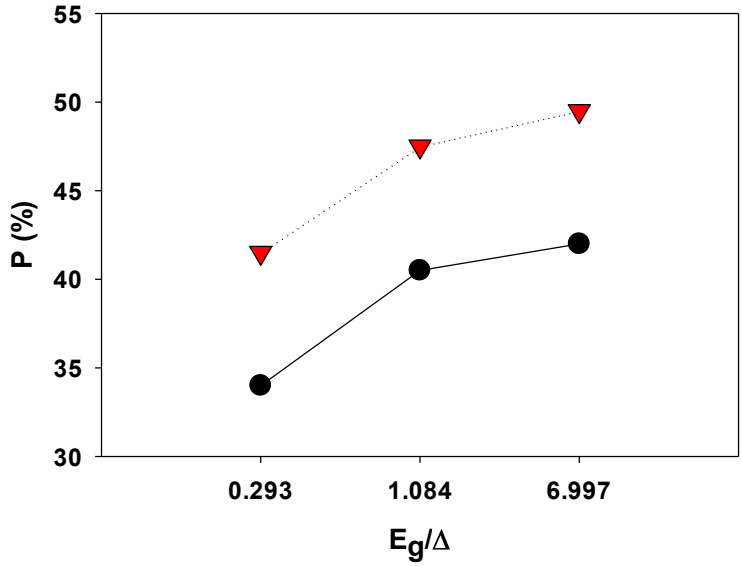

Fig. (7) Spin-polarization as a function of E_g/Δ for the excess photon energy of 200 meV, excited by one-photon (circle) and two-photon (triangle) excitations.

5. Conclusions

Single-colour multiphoton spectroscopy, spin generation and spin polarization in noncentrosymmetric InSb, GaSb and ZnSe were investigated on the basis of the Kane model. It was found that the electronic spin polarization depends on the excitation scheme of the spectroscopy as well as the excess photon energy of exciting carriers. A maximum value of *P* was found to be about 55%. The *P* reaches its maximum value at the lower energy and sustains shorter energy range for InSb. The *P* was also found to depend on the bandgap energy and spin-orbit splitting. On comparison, it was clear that the multiphoton spectroscopy enhances the electron spin generation and polarization over single-photon absorption in these compounds. The possible reasons were discussed. The results were also discussed on the basis of dominant spin relaxation mechanism.

References

[1] G.A. Prinz, Science 282, 1660 (1998).
[2] M.I. Dyakonov and A.V. Khaetskii, **"Spin Hall Effect",** in **Spin Physics in Semiconductors**, M.I. Dyakonov, Ed., Springer-Verlag, Berlin (2008).
[3] D.D. Awschalom, D. Loss, and N. Samarth, **"Semiconductor Spintronics and Quantum Computation"**, Eds., Springer, Berlin (2002).
[4] M.I. Miah, Appl. Phys. Lett. 92, 092104 (2008).
[5] M.I. Miah, J. Optoelectron. Adv. Mater. 10, 2487 (2008).
[6] M.N. Biabich et al., Phys. Rev. Lett. 61, 2472 (1988).
[7] G. Binasch et al., Phys. Rev. B. 39, 4828 (1989).
[8] H. Akinaga and H. Ohno, IEEE Trans. Nanotechnol. 1, 19 (2002).
[9] M.I. D'yakonov, Spintronics? in: S. Luryi, J. Xu, and A. Zaslavsky (Eds.), **"Future Trends in Microelectronics: the Nano, the Giga and the Ultra"**, Wiley-IEEE Press, New York (2004).
[10] D.T. Pierce and F. Meier, Phys. Rev. B 13, 5484 (1976).
[11] M.I. Miah and E. MacA. Gray, Curr. Opin. Solid State Mater. Sci. 14, 49 (2010).
[12] E.L. Ivchenko, **"Optical spectroscopy of semiconductor nanostructures"**, Harrow, Alpha Science Int. (2005).
[13] M.I. Miah, Opt. Commun. 284, 1254 (2011).
[14] M.I. Miah, Mater. Chem. Phys. 128, 548 (2011).
[15] A.M. Danishevskii et al., Sov. Phys. JETP 16, 440 (1972).
[16] G. Lampel and C. Weisbuch, Solid State Comm. 16, 877 (1975).
[17] M. Cardona, N.F. Christensen, and G. Fasol, Phys. Rev. B 38, 1806 (1988).
[18] E.O. Kane, J. Phys. Chem. Solids 1, 249 (1957).
[19] M.I. Miah, J. Phys. Chem. B, 6800 (2009).
[20] H. Mayer and U. Rossler, Solid State Commun. 87, 81 (1993).
[21] M.I. Miah, J. Appl. Phys. 103, 123711 (2008).
[22] I.V. Kityk, Phys. Solid State 33, 1026 (1991).
[23] M. Salimullah et al., J. Phys. D: Appl. Phys. 36, 958 (2003).
[24] G.E. Pikus, and A.N. Titkov, in: F. Meier and B. P. Zakharchenya (Eds.), Optical Orientation, Modern Problems in Condensed Matter Science, Vol. 8, North-Holland, Amsterdam, 1984.